Efficiency of pump absorption in double-clad fiber amplifiers. III. Calculation of modes

Dmitrii Kouznetsov and Jerome V. Moloney

Arizona Center for Mathematical Sciences, Department of Mathematics, University of Arizona, 617 North Santa Rita, Tucson, Arizona 85721

Received April 27, 2001; revised manuscript received July 23, 2001

Using an analogy with quantum mechanics we employ a technique that enables us to calculate the efficiency of an incoherent pump in general-geometry double-clad fibers. This approach yields accurate estimates of the absorption rate of each mode of the pump in the first order of perturbation theory. Such estimates are compared with results of numerical simulations reported recently. The comparison confirms the high efficiency of a spiral-shaped cladding. © 2002 Optical Society of America

OCIS codes: 140.3510, 060.2320, 060.0060.

1. INTRODUCTION

The high efficiency of fiber amplifiers[1–4] makes the amplification coefficient (for a weak input signal) and the output power (for a strong input signal) almost proportional to the power of the pump absorbed in the fiber. For double-clad amplifiers, an appropriate configuration of the core and cladding should provide effective coupling of the pump light into the core. Analysis of the efficiency of the absorption of pump light in double-clad fibers is important for the optimization of fiber amplifiers.

With good coupling, the effective absorption rate of the pump can be estimated as $\mathcal{K}_{\text{eff}} = v\sigma_0 s/(s + S)$, where v is the concentration of the active centers, σ_0 is the cross section of the absorption, s is the area of core, and S is the area of the cladding. The concentration v cannot be too high because of collective effects.[5] The area s should be small enough to support single-mode propagation of the signal. The area S should be large enough to enable good coupling at the input of the multimode pump into the cladding. So, the geometry of the double-clad fiber should provide the maximum absorption of the pump in the core for a given concentration v and given cross sections σ_0, s, S.

For simple-geometry double-clad fibers, geometrical optics[6–8] gives satisfactory estimates of the efficiency of absorption of the pump light in the core. This agrees with experiment[9] and with results of the wave-optical approach.[10] In previous papers[10,11] we described the method of approximate images (AIs), which allows for numerical simulations of the paraxial scalar equation of diffraction using the fast Fourier transform. It was shown that a small spiral deformation of a circular cladding can be as efficient as strong cuts[12] for the mixing of the incoherent pump light. Simulations with AIs are not efficient if the absorption rate $\mathcal{K}$ is small in comparison with $1/L_{\text{dif}}$, the rate of change of the structure of the field due to diffraction. It should be noted that this case is realized in existing fiber amplifiers. This can be seen from the following estimates. The highest signal gain of the order of 5 dB/cm reported[13,14] corresponds to a rate of the absorption of the field of the pump of the order of $\mathcal{K}_0 \approx 1\ \text{cm}^{-1}$. Usually the effective absorption rate is several orders of magnitude lower. At the same time, the effective rate of change L_{dif}^{-1} of the structure of the field of the pump that is due to diffraction in double-clad fibers can be estimated as a product of the numerical aperture and the wave number $k = 2\pi n_0/\lambda$. This gives values of the effective rate of change of the structure of the pump of $\sim 10^4\ \text{cm}^{-1}$, which is at least 4 orders of magnitude greater than the effective absorption rate. The asymptotic behavior of the efficiency of absorption of the pump light at realistic (i.e., small) values of $\mathcal{K}_0 L_{\text{dif}}$ can be revealed from the simulations of Refs. 10 and 11. The effective rate of absorption of the pump is almost proportional to the local absorption rate.[6,10–12] Such proportionality indicates that the effective absorption rate can be calculated in the first order of perturbation theory without having to deal with eigenfunctions of non-Hermitian operators.[15] First, modes of the unperturbed (without absorption) fiber will be calculated. Next, the effective operator of propagation will be diagonalized. This is done numerically in this paper.

The usual finite difference approximation of the second-order differential operator appearing in the paraxial-equation description of the fiber waveguide leads to an ill-posed problem. In this case, the largest nondiagonal elements of the resulting matrix are insensitive to the distribution of the index of refraction in the fiber: We would have to apply extremely high-accuracy arithmetics, at least, to avoid the loss of information about the structure of the fiber at the first steps of the procedure of diagonalization. To avoid this difficulty, we expand both Hamiltonian and eigenmodes in some system of smooth basis functions. Sinusoidal harmonics allow us to employ fast sine-transform algorithms, and we take into account a finite set of sinusoidal harmonics. This corresponds to some smooth truncation of the Hamiltonian. A similar approach was analyzed in Ref. 16 mathematically; it was shown that the error of such an approximation decreases faster than the inverse power of the number of harmonics taken into account.

The result of approximations using an eigenfunction

expansion will be compared with a direct numerical method. Comparison will be made for the efficiency of coupling of the pump light into the core. We calculate this efficiency by using the decoherence approximation within the framework of the eigenfunction expansion of the Hamiltonian and compare it with the results of the direct simulations with the AI method.[10,11]

2. HAMILTONIAN AND DECOHERENCE APPROXIMATION

Light propagation in a medium with variations of the dielectric constant ϵ is described by Maxwell's equations

$$\operatorname{curl}\mathbf{E} = -\frac{1}{c}\dot{\mathbf{H}}, \tag{1}$$

$$\operatorname{curl}\mathbf{H} = \frac{\epsilon}{c}\dot{\mathbf{E}} + 4\pi\sigma\mathbf{E}, \tag{2}$$

where $\mathbf{E}$ and $\mathbf{H}$ are the electric and magnetic fields, c is the velocity of light, and we assume that the magnetic susceptibility is equal to unity. Taking the curl of Eq. (1), interchanging the order of the time derivative (dot) and curl, and neglecting the term with the divergence gradient, div **grad**, we get the wave equation

$$-\nabla^2\mathbf{E} = -\frac{\epsilon}{c^2}\ddot{\mathbf{E}} + \frac{4\pi\sigma}{c}\dot{\mathbf{E}}.$$

For each spectral component of the field $\mathbf{E} = \operatorname{Re}\Sigma_{\omega,\mathbf{e}}\mathbf{e}E_{\omega,\mathbf{e}}\exp(-i\omega t)$ we have the scalar equation

$$-\nabla^2 E = \frac{\mu\epsilon}{c^2}\omega^2 E + \frac{4\pi}{c}\sigma(-i\omega)E,$$

where $E = E_{\omega,\mathbf{e}}$. Setting $\omega/c = k_0 =$ constant, we get $\nabla^2 E + \epsilon k_0^2 E = -i4\pi\sigma k_0 E$. In the paraxial limit, setting $E = f(x, y, z)\exp(ikz)$ and neglecting terms involving $\partial^2 f/\partial z^2$, we obtain the following equation:

$$f' = \frac{1}{2ik}[-\Delta_\perp + (k^2 - \epsilon k_0^2)]f - \frac{2\pi\sigma k_0}{k}f, \tag{3}$$

where

$$\Delta = \frac{\partial^2}{\partial x^2} + \frac{\partial^2}{\partial y^2}, \qquad f' = (x, y, z)/\partial z.$$

Define the Hamiltonian

$$\mathcal{H} = -\Delta + U, \tag{4}$$

where $U = k^2 - \epsilon k_0^2$ can be interpreted as a potential of a single particle in a two-dimensional quantum system. The parameter $\mathcal{K} = 2\pi\sigma k_0/k$ should be interpreted as the local absorption rate. The evolution of the field of the pump can be written as follows:

$$f' = \frac{1}{2ik}\mathcal{H}f - \mathcal{K}f. \tag{5}$$

Assume that $f(x, y, 0)$ is given. How do we find the distribution $f(x, y, z)$? Let $\{\psi_n, n = 1, 2,\ldots\}$ be a set of the normalized eigenfunctions of the Hamiltonian $\mathcal{H}$. Then, by analogy with quantum mechanics, the field f can be expanded with respect to these functions:

$$f = \sum_n C_n\psi_n \exp\left(\frac{1}{2ik}\mathcal{E}_n z\right), \tag{6}$$

where $\mathcal{E}_n$ $\{n = 1, 2,\ldots\}$ are the corresponding eigenvalues and $\mathcal{H}\psi_n = \mathcal{E}_n\psi_n$. In the absence of absorption, $C_n =$ constant, and the expansion of f at $z = 0$ gives the solution for any z.

In the presence of absorption, we should consider the evolution equations for the expansion coefficients C_n:

$$C_m'(z) = -\sum_n \mathcal{K}_{m,n}\exp\left[\frac{i}{2k}(\mathcal{E}_m - \mathcal{E}_n)z\right]C_n, \tag{7}$$

where

$$\mathcal{K}_{m,n} = \int \mathrm{d}x\,\mathrm{d}y\,\mathcal{K}\psi_m\psi_n. \tag{8}$$

(We have no need to take the conjugation of the mode ψ in Eq. (8) as the modes can be taken as real functions.)

The typical value of $2k/|\mathcal{E}_m - \mathcal{E}_n|$ is the diffraction length of the field. (At such a length of propagation, the structure of the field changes significantly owing to diffraction.) For multimode fibers with a wide aperture, such a length can be several wavelengths, i.e., approximately a few micrometers.

We expect the absorption in the core of a fiber amplifier to be significant at lengths of the order of 1 cm or more, even for the extremely high concentrations of the amplifying dopant.[13,14] Thus the exponentials in Eq. (7) oscillate very quickly in comparison with the variation of coefficients C_n. Then only the case with $m = n$ in the sum is significant. Neglecting rapidly oscillating terms, we write simply

$$C_m' = -\mathcal{K}_{m,m}C_m. \tag{9}$$

In this approximation, each mode ψ decays with its own rate, independently of other modes. (In the case of a degenerate spectrum, for example, due to some symmetry, we need to redefine the degenerate eigenfunctions in such a way as to eliminate the off-diagonal matrix elements of $\mathcal{K}$.) There is therefore no need to solve the system of Eq. (7), and we can consider the uncoupled Eq. (9) instead, which has the solution

$$C_m(z) = \exp(-\mathcal{K}_{m,m}z)C_m(0). \tag{10}$$

Now assume that the initial power of the pump is distributed uniformly among the first L modes. Then the efficiency of coupling of this power into the core can be estimated as follows:

$$\eta = 1 - \frac{1}{L}\sum_{m=1}^{L}\exp(-2\mathcal{K}_{m,m}z). \tag{11}$$

In addition to the analytic estimates of the validity of the approximation above, it would be interesting to compare such an estimate to an independent calculation. In Sections 4 and 5, we compare the estimate of Eq. (11) to results of the direct simulation of the propagation of a paraxial pump.[11] Before this we describe the procedure for the evaluation of the diagonal elements of the matrix $\mathcal{K}$, with the simplest way being to diagonalize the Hamiltonian $\mathcal{H}$. This will be subject of Section 3.

3. DIAGONALIZATION OF HAMILTONIAN

The standard numerical approach is to discretize the Laplacian operator by use of a finite difference mesh. The resulting matrix problem can be treated with the methods of linear algebra. The disadvantages of such an approach are discussed in Section 1. To avoid in ill-posed problem, we expand the modes ψ by using a set of harmonic basis functions

$$F_{\mathbf{j}}(x, y) = \frac{2}{(AB)^{1/2}} \sin\frac{\pi m x}{A} \sin\frac{\pi n y}{B}, \tag{12}$$

where $\mathbf{j} = \{m, n\}$, $m = 1, 2, \ldots,$ and $n = 1, 2, \ldots$. Constants A and B define the size of the box in which the eigenfunctions will be reconstructed. Physically such a box is equivalent to a potential gap with infinite potential walls, or to an ideally reflecting surface of the rectangular outer cladding.

We approximate the Hamiltonian [Eq. (4)] with respect to the basis [Eq. (12)]. The representation of the operator $-\Delta$ is trivial:

$$\langle F_{\mathbf{j}_1} | -\Delta | \mathbf{F}_{\mathbf{j}_2} \rangle = \delta_{\mathbf{j}_1,\mathbf{j}_2} \left[\left(\frac{\pi}{A} m \right)^2 + \left(\frac{\pi}{B} n \right)^2 \right]. \tag{13}$$

For the representation of the potential, we apply the trigonometric formula $2 \sin z_1 \sin z_2 = \cos(z_1 - z_2) - \cos(z_1 + z_2)$ to yield

$$\begin{aligned} U_{\mathbf{j}_1,\mathbf{j}_2} &= \langle F_{\mathbf{j}_1} | U | F_{\mathbf{j}_2} \rangle \\ &= \frac{1}{MN} \int \mathrm{d}\mu \mathrm{d}\nu \left(\cos\frac{\pi(m_1 - m_2)\mu}{M} - \cos\frac{\pi(m_1 + m_2)\mu}{M} \right) \\ &\quad \times \left(\cos\frac{\pi(n_1 - n_2)\nu}{N} - \cos\frac{\pi(n_1 + n_2)\nu}{M} \right) U\left(\frac{A\mu}{M}, \frac{B\nu}{N} \right). \end{aligned}$$

Replacing the integrals with discrete sums, we write

$$\begin{aligned} U_{\mathbf{j}_1,\mathbf{j}_2} \approx \frac{1}{MN} (&\mathcal{U}_{m_1 - m_2, n_1 - n_2} - \mathcal{U}_{m_1 - m_2, n_1 + n_2} \\ &- \mathcal{U}_{m_1 + m_2, n_1 - n_2} + \mathcal{U}_{m_1 + m_2, n_1 + n_2}), \end{aligned} \tag{14}$$

where

$$\mathcal{U}_{m,n} = \sum_{\mu,\nu} \cos\frac{\pi m \mu}{M} \cos\frac{\pi n \nu}{N} U\left(\frac{A\mu}{M}, \frac{B\nu}{N} \right). \tag{15}$$

Formulas (12)–(15) define the four-subscript matrix $\tilde{\mathcal{H}}_{\mathbf{j}_1,\mathbf{j}_2} = \langle F_{\mathbf{j}_1} | - \Delta | F_{\mathbf{j}_2} \rangle + U_{\mathbf{j}_1,\mathbf{j}_2}$ in the space of $(M/2) \times (N/2) \times (M/2)(N/2)$ wave vectors. We take into account only components with transversal wave number $\mathbf{p} = \{p_x, p_y\}$ such that $|\mathbf{p}| \leqslant k_{\max} = \text{constant}$. To each component we assign a single index j so that we avoid working with four-index matrices. We then diagonalize the restricted $J \times J$ matrix $\mathcal{H}$ with elements

$$\mathcal{H}_{a,b} = \langle F_a | H | F_b \rangle. \tag{16}$$

Each element is related to the four-index matrix $\tilde{\mathcal{H}}$ through the simple expression $\tilde{\mathcal{H}}_{\{m,n\},\{m_1,n_1\}} = \mathcal{H}_{j_{m,n} j_{m_1,n_1}}$. The diagonalization returns an approximation to the eigenvalues $\mathcal{E}$ and the unitary matrix S such that

$$(S \mathcal{H} S^{\dagger})_{a,b} = \mathcal{E}_b \delta_{a,b}, \qquad S S^{\dagger} = 1. \tag{17}$$

For each fixed b, $S_{a,b}$ can be interpreted as an approximation of the eigenfunction of the Hamiltonian in the momentum representation:

$$\sum_{m_2,n_2} \mathcal{H}_{j_{m_1,n_1}, j_{m_2,n_2}} S_{j_{m_2,n_2},b} = \mathcal{E}_b S_{j_{m_1,n_1},b}. \tag{18}$$

The eigenmodes of the fiber can be reconstructed as the sine transform of S:

$$\psi_b\left(\frac{A\mu}{M}, \frac{B\nu}{N} \right) = \sum_{m,n} \sin\frac{\pi m \mu}{M} \sin\frac{\pi n \nu}{N} S_{j_{m,n},b}. \tag{19}$$

Equation (19) approximates the eigenfunction of the Hamiltonian for $b \ll J$, i.e., while the number L of modes we calculate is small compared with the number J of basis functions we used in the expansion. (All eigenfunctions are sorted by the eigenvalues.) In the examples below, we take into account as many as 1800 basis functions. We were able to calculate several hundred modes accurately with such a basis. In this case, the diagonalization took several hours on a single processor of a Silicon Graphics ONYX2 running at 300 MHz. Such a run time is comparable with the simulation time of a single realization by the AI method described in Refs. 10 and 11.

The algorithm above allows one to approximate the eigenfunctions of the Hamiltonian $\mathcal{H}$ accurately by using the harmonic basis. In Sections 4 and 5 we apply the procedure above to calculate the efficiency of coupling of pump power in fibers with different geometries.

4. FIBER WITH CIRCULAR SYMMETRY

The fiber with circular symmetry is a good test example of the algorithm described above. Modes of the circular fiber are highly symmetric, and any violation of the symmetry would indicate limits of applicability of the approximate eigenmodes.

Define the cylindrical coordinates ρ, ϕ such that $x = \rho \cos\phi$, $y = \rho \sin\phi$. Let the dielectric constant be $\epsilon = \epsilon_1 = n_1^{1/2}$ in the core (i.e., $\rho < r_0$), and $\epsilon = \epsilon_2 = n_2^{1/2}$ in the cladding ($\rho > r_0$). At the given wave number k, this corresponds to the effective potential $U_1 = U_0 + \epsilon_1 k_0^2 = \text{constant}$ in the core and $U_2 = U_0 + \epsilon_2 k_0^2 = \text{constant}$ in the cladding. Also, we need to include some external cladding with a high enough potential $U_3 = \text{constant}$ to approximate the boundary condition $E = 0$ at $\rho = R_0$. To improve the approximation, we smooth the potential at the scale of the step d_x of the grid:

$$U = \frac{U_1}{1 + \exp[(\rho - r_0)/d_x]} + \frac{U_3}{1 + \exp[(R_0 - \rho)/d_x]}. \tag{20}$$

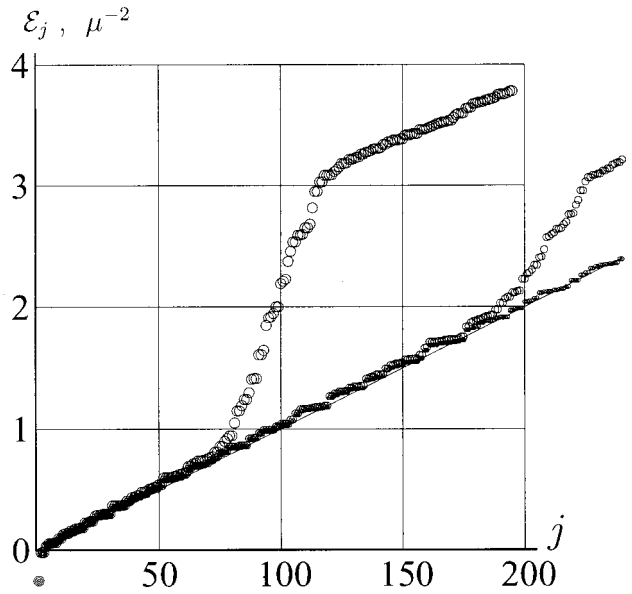

Fig. 1. Eigenvalues versus number of eigenfunctions for the circular double-clad fiber, estimated with $k_{\max} = 1\ \mu\mathrm{m}^{-1}$, 195 basis functions, large circles; $k_{\max} = 1.5\ \mu\mathrm{m}^{-1}$, 447 basis functions, medium circles; $k_{\max} = 2\ \mu\mathrm{m}^{-1}$, 803 basis functions, small circles; $k_{\max} = 3\ \mu\mathrm{m}^{-1}$, 1830 basis functions, dots. The solid line represents the estimate $\mathcal{E}_n = (kR_0)^2 n$.

The choice $r_0 = 4\ \mu\mathrm{m}$, $R_0 = 20\ \mu\mathrm{m}$, $U_1 = -0.44\ \mu\mathrm{m}^{-2}$, $U_2 = 0$, and $k = 10\ \mu\mathrm{m}^{-1}$ corresponds to the fiber simulated in Ref. 11 with an AI. We take $U_3 = 3\ \mu\mathrm{m}^{-2}$ to make our modes decay efficiently outside of the inner cladding. Physically, this situation corresponds to the pump with wavelength $\lambda = 2\pi/k_0 = 0.98\ \mu\mathrm{m}$, with $n_0 = 1.5$, $n_1 = n_0 + 0.0033$, $n_2 = n_0$, $n_3 = n_0 - 0.0225$.

Figure 1 shows the first hundred eigenvalues of the operator $\mathcal{H}$ estimated with different J. This calculation corresponds to $A = B = 51.2\ \mu\mathrm{m}$, $d_x = d_y = 0.2\ \mu\mathrm{m}$ at $k_{\max} = 1\ \mu\mathrm{m}^{-1}$, large circles; $k_{\max} = 1.5\ \mu\mathrm{m}^{-1}$, intermediate circles; $k_{\max} = 2\ \mu\mathrm{m}^{-1}$, small circles; $k_{\max} = 3\ \mu\mathrm{m}^{-1}$, dots. For each case the corresponding number of basis functions taken into account are $J = 195$, 447, 803, 1830. Eigenvalues estimated in the last two cases are so close that the difference is hard to see at the resolution of the graphics. We estimate that we have at least 300 correctly approximated modes.

The solid curve corresponds to the asymptotic estimate

$$\mathcal{E}_j = 4j/(kR_0)^2, \tag{21}$$

which ignores the core.

The efficiency of the coupling of the power of the pump into the core can be estimated from Eq. (11). This estimate is compared with results obtained by other methods in the lower group of curves in Fig. 2, which represent the efficiency versus dimensionless $Z = \mathcal{K}_0 z$ for various cases. The lowest dashed curve represents the analytical estimate based on geometrical optics[10–12]; the curve with vertical bars represents the results of simulation of one realization of the field with an AI. These two curves are the same as in Fig. 2 of Ref. 11. Solid curves represent the estimate by Eq. (20) with various number L of modes. The lowest curve corresponds to $L = 300$, the intermediate to $L = 200$ and the upper to $L = 100$. Although the distribution of initial power among the modes in the chaotic field used in Ref. 11 is not exactly uniform, the estimate with 300 modes shows good agreement between the two methods. We expect that as both the refractive index step $n_2 - n_3$ and the number L of modes increase, the estimate according to Eq. (11) will approach the lowest dashed curve, which corresponds, as noted above, to the limit of geometrical optics.

Note that the modes taken into account in this paper are located mainly within the inner cladding. However, for large numbers of modes and given $n_2 - n_3$, the highest modes tend to fill the full computational domain. Then the efficiency of absorption of the pump light begins to depend on the sizes A and B of this domain. Walls of the domain cause some additional concentration of pump light, increasing the efficiency. Physically, this could describe the role of rectangular outer cladding. In the simulations described here, the numerical aperture of the input signal is not greater than 0.1. At $n_2 - n_3 = 0.0225$, most of the modes are localized inside the inner cladding and decay fast outside. For these modes, the step between the inner and the outer cladding acts like a mirror. This is why one observes good agreement between calculations based on simulations using AIs and the estimate based on the mode expansion [Eq. (11)].

5. SPIRAL CLADDING

The example of the previous section is important as a test of the algorithm of diagonalization of the Hamiltonian.

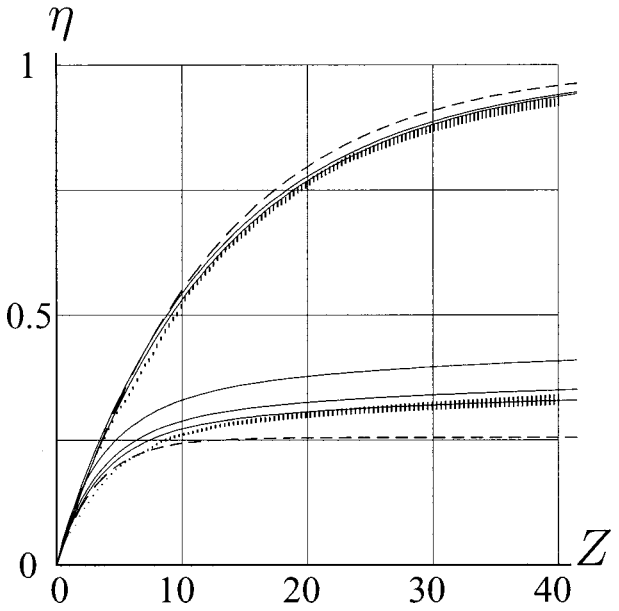

Fig. 2. Efficiency η versus dimensionless length of propagation $Z = \mathcal{K}_0 z$. The lower group of curves corresponds to the fiber with circular symmetry; dashed curve, estimate on basis of geometric optics[10,11]; vertical bars, AI simulation[11]; solid curves, calculations based on first order perturbation theory with respect to $\mathcal{K}_0$ by Eq. (11) with $J = 300$ (lowest), $J = 200$ (intermediate), $J = 100$ (highest). The same conditions as in Fig. 1, i.e., 1830 basis functions, were used to diagonalize the Hamiltonian. The upper group of curves corresponds to the fiber with spiral cladding by Eq. (22) and offset core; dashed curve, case of ideal mixing of pump,[10,11] $\eta = 1 - \exp[-2\mathcal{K}_0(r_0/R_0)^2 z]$; vertical bars, AI simulation.[11] Two solid curves represent the first order perturbation theory calculations showing the first 150 modes (upper) and first 300 modes (lower).

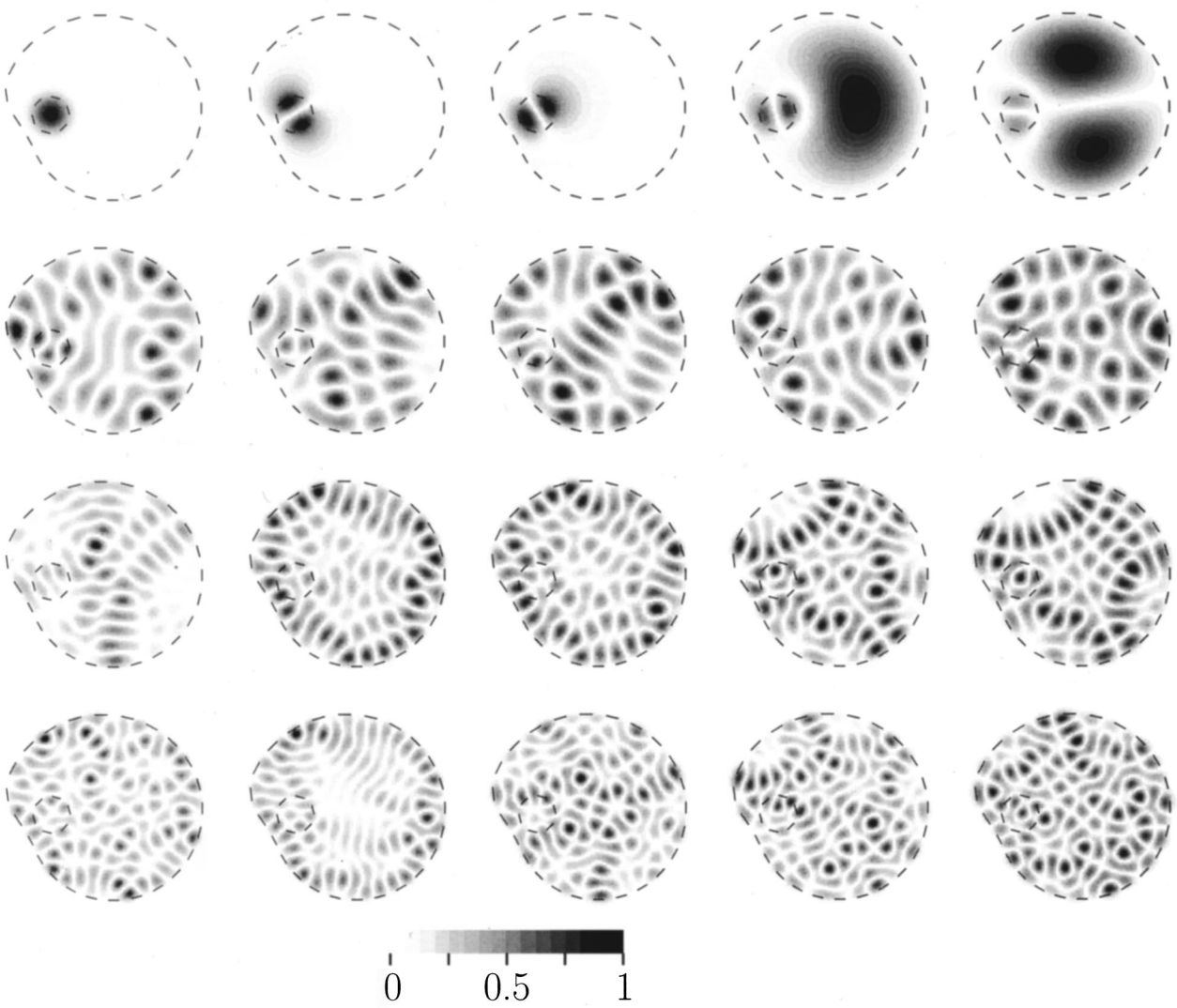

Fig. 3. Distribution of amplitude of modes of spiral fiber with offset core. Modes 1–5, 51–55, 101–105, 151–155 are shown top row to bottom row. Dashed outlines indicate the core and the cladding.

For practical applications, the case with broken symmetry is more interesting, as asymmetric fibers provide more efficient coupling of pump power into the core.

In this section we consider the same smooth spiral fiber as in Ref. 11 and compare the results using diagonalization of the Hamiltonian with results using simulations with AIs.

Let the surface of the cladding be parameterized in polar coordinates by the function $R(\phi)$. The choice

$$R(\phi)=\begin{cases} R_0+\alpha_0\phi, & |\phi|\le\beta_0 \\ R_0+\alpha_0\sin\phi\left[\dfrac{\pi+\beta_0}{\pi-\beta_0}(\pi-|\phi|)-\dfrac{\pi}{(\pi-\beta_0)^2}(\pi-|\phi|)^2\right], & |\phi|\ge\beta_0, \end{cases} \quad (22)$$

corresponds to Eq. (13) and Fig. 2(a) of Ref. 11 at $\alpha_0 = 1\,\mu$m, $\beta_0 = 2.7$ rad and coordinates of the center of the core $x_0 = -12\,\mu$m, $y_0 = 0$. Other parameters are the same as in the example of the previous section, except that in Eq. (20), we replace R_0 with $R(\phi)$. Some modes of such a fiber are shown in Fig. 3. Darker regions correspond to larger amplitude of the field, according to the scale of relative amplitudes plotted at the bottom of Fig. 3. In this figure the normalization $\mathrm{Max}_{x,y}|\Psi(x,y)| = 1$ is used. Note the similarity in the texture of modes in Fig. 3 and the speckle pattern shown in Fig. 1(b) of Ref. 12.

The estimate of the efficiency of coupling of the pump power into the core by Eq. (11) for such a fiber is compared with the results of the numerical simulations with AIs[11] in the upper group of curves in Fig. 2. Parameters are the same as in Fig. 1. The upper dashed curve rep-

resents the analytical estimate $\eta = 1 - \exp(2\mathcal{K}_0 r_0^2/R_0^2 z)$ from Refs. 10–12 and corresponds to the case of ideal mixing of the pump. Vertical bars correspond to the numerical simulation by the AI method; they reproduce the bar curve from Fig. 2(b) of Ref. 11. (In that paper, the maximum transversal wave number was 2 μm^{-1} at the initial stage of generation of incident field; this would correspond to $J = 400$ at the given value of R_0. However, the multiple iterations necessary to adjust this field to the fiber slightly reduced the amount of effectively excited modes, so the effective numerical aperture was ~0.15.)

Solid curves represent the case of the pump light distributed uniformly among the first 150 modes (upper solid curve) and the case with 300 modes (solid curve slightly below and which nearly coincides with the previous curve). The difference is very small, and all these curves are close to the case of the ideal mixing of modes. This confirms the good mixing of the pump light in a fiber with spiral cladding mentioned in Ref. 11. The efficiency of absorption of pump light is only 4% less than in the case of ideal mixing. Note that the chaotic double-truncated fiber[12] also shows an efficiency 4% less than the ideal case. The cladding with small spiral distortion[11] seems to be more practical than the double-cut fiber,[12] with respect to both fabrication and coupling to the source of a multimode pump.

6. CONCLUSIONS

The propagation of a multimode pump in a double-clad fiber is considered in the paraxial approximation. The absorption of the pump light in the core is estimated in the first order of perturbation theory by use of an analogy with quantum mechanics. This leads to the simple estimate of Eq. (11) for the efficiency of coupling of the pump light into the core. This estimate is compared with the numerical simulations[11] reported recently. Figure 2 shows good agreement between both approaches. The approximation developed seems to be valid for all reported fiber amplifiers, even for the case of the highest acceptable concentrations of active centers in the core.[13,14]

ACKNOWLEDGMENTS

The authors thank E. M. Wright, R. M. Indik, M. Kolesik, M. Brio, A. Zakharian and other colleagues from the Arizona Center for Mathematical Sciences for their help and discussions. This work was supported by Air Force Office of Scientific Research grants F49620-00-1-0002 and F49620-00-1-0190, and in part by National Science Foundation Grant/Opportunities for Academic Liaison with Industry/Division of Mathematical Sciences 9811466.

D. Kouznetsov's e-mail address is dima @acms.arizona.edu.

REFERENCES

1. K. Ueda and A. Liu, "Future of high-power fiber lasers," Laser Phys. **8**, 774–781 (1998).
2. V. Dominic, S. MacCormack, R. Waarts, S. Sanders, S. Bicknese, R. Dohle, E. Wolak, P. S. Yeh, and E. Zuker, "110 W fiber laser," Electron. Lett. **35**, 1158–1160 (1999).
3. N. S. Kim, T. Hamada, M. Prabhu, C. Li, J. Song, K. Ueda, A. P. Liu, and H. J. Kong, "Numerical analysis and experimental results of output performance for Nd-doped double-clad fiber lasers," Opt. Commun. **180**, 329–337 (2000).
4. C. K. Liu, F. S. Lai, and J. J. Jou, "Analysis of nonlinear response in erbium-doped fiber amplifiers," Opt. Eng. **39**, 1548–1555 (2000).
5. T. Ohtsuki, S. Honkanen, S. I. Najafi, and N. Peyghambarin, "Cooperative upconversion effects on the performance of the Er^{3+}-doped phosphate glass waveguide amplifiers," J. Opt. Soc. Am. B **14**, 1838–1845 (1997).
6. A. Liu and K. Ueda, "The absorption characteristics of circular, offset, and rectangular double-clad fibers," Opt. Commun. **132**, 511–518 (1996).
7. P. Leproux, S. Février, V. Doya, P. Roy, and D. Pagnoux, "Modeling and optimization of double-clad fiber amplifiers using chaotic propagation of pump," Opt. Fiber Technol. **6/7**, 324–339 (2001).
8. C. L. Bonner, T. Bhutta, D. P. Shepherd, and A. C. Tropper, "Double-clad structures and proximity coupling for diode-bar-pumped planar waveguide lasers," IEEE J. Quantum Electron. **36**, 236–242 (2000).
9. S. Bedö, W. Lüthy, and H. P. Weber, "The effective absorption coefficient in double-clad fibers," Opt. Commun. **99**, 331–335 (1993).
10. D. Kouznetsov, J. V. Moloney, and E. M. Wright, "Efficiency of pump absorption in double-clad fiber amplifiers. I. Fiber with circular symmetry," J. Opt. Soc. Am. B **18**, 743–749 (2001).
11. D. Kouznetsov and J. V. Moloney, "Efficiency of pump absorption in double-clad fiber amplifiers. II. Broken circular symmetry," J. Opt. Soc. Am. B **19**, 1259–1263 (2002).
12. V. Doya, O. Legrand, and F. Mortessagne, "Optimized absorption in a chaotic double-clad fiber amplifier," Opt. Lett. **26**, 872–874 (2001).
13. Y. C. Yan, A. J. Faber, H. de Waal, P. G. Kik, and A. Polman, "Erbium-doped phosphate glass waveguide on silicon with 4.1 dB/cm gain at 1.535 μm," Appl. Phys. Lett. **71**, 2922–2924 (1997).
14. Y. Hu, S. Jiang, T. Luo, K. Seneshal, M. Morell, F. Smektala, S. Honkanen, J. Lucas, and N. Peyghambarian, "Performance of high-concentration Er^{3+}-Yb^{3+}-codoped phosphate fiber amplifiers," IEEE Photonics Technol. Lett. **13**, 657–659 (2001).
15. S. L. Lin, L. W. Li, T. S. Yeo, and M. S. Leong, "QZ factorization for generalized eigenvalues applied to waveguide analysis," Microwave Opt. Technol. Lett. **28**, 361–364 (2001).
16. A.-S. Bonnet-Bendhia and N. Gmati, "Spectral approximation of a boundary condition for an eigenvalue problem," SIAM J. Numer. Anal. **32**, 1263–1279 (1995).